Molecular Biology of the Cell
Vol. 19, 4628–4639, November 2008

Membrane Ruffles Capture C3bi-opsonized Particles in Activated Macrophages

Prerna C. Patel* and Rene E. Harrison*†

*Departments of Biological Sciences and †Cell and Systems Biology, University of Toronto Scarborough, Toronto, ON, M1C 1A4, Canada

Submitted February 29, 2008; Revised August 12, 2008; Accepted August 27, 2008
Monitoring Editor: Jennifer Lippincott-Schwartz

A widespread belief in phagocyte biology is that FcγR-mediated phagocytosis utilizes membrane pseudopods, whereas Mac-1–mediated phagocytosis does not involve elaborate plasma membrane extensions. Here we report that dynamic membrane ruffles in activated macrophages promote binding of C3bi-opsonized particles. We identify these ruffles as components of the macropinocytosis machinery in both PMA- and LPS-stimulated macrophages. C3bi-particle capture is facilitated by enrichment of high-affinity Mac-1 and the integrin-regulating protein talin in membrane ruffles. Membrane ruffle formation and C3bi-particle binding are cytoskeleton dependent events, having a strong requirement for F-actin and microtubules (MTs). MT disruption blunts ruffle formation and PMA- and LPS-induced up-regulation of surface Mac-1 expression. Furthermore, the MT motor, kinesin participates in ruffle formation implicating a requirement for intracellular membrane delivery to active membrane regions during Mac-1–mediated phagocytosis. We observed colocalization of Rab11-positive vesicles with CLIP-170, a MT plus-end binding protein, at sites of particle adherence using TIRF imaging. Rab11 has been implicated in recycling endosome dynamics and mutant Rab11 expression inhibits both membrane ruffle formation and C3bi-sRBC adherence to macrophages. Collectively these findings represent a novel membrane ruffle "capture" mechanism for C3bi-particle binding during Mac-1–mediated phagocytosis. Importantly, this work also demonstrates a strong functional link between integrin activation, macropinocytosis and phagocytosis in macrophages.

INTRODUCTION

Diverse cellular mechanisms have evolved to allow internalization of large particles and entire cells into the cytoplasm of another cell. Bacteria are particularly specialized in penetrating host cells (Isberg, 1991; Bliska *et al.*, 1993). For instance, *Yersinia* binds to host β1-integrins to induce receptor-mediated uptake (Dersch and Isberg, 1999). Numerous other bacteria, including *Salmonella* spp., inject proteins into the cytoplasm of host cells to provoke membrane ruffling and macropinocytosis, termed "triggered phagocytosis" (Jones *et al.*, 1993; Garcia-del Portillo and Finlay, 1994; Finlay and Cossart, 1997). Internalization of these bacteria into host cells shields them intracellularly from patrolling immune cells.

In mammals, phagocytes are specialized cells that are fully equipped to engulf other cells into their cytoplasm. The phagocytes include macrophages and neutrophils, which express a broad spectrum of receptors that participate in target cell recognition and internalization. Fcγ receptors bind to immunoglobulin G (IgG), and complement receptors (CRs) recognize C3bi-opsonized targets. Detailed signaling events during FcγR-mediated phagocytosis that lead to plasma membrane pseudopod extension and particle engulfment have been elucidated (Cox *et al.*, 2000). Fcγ receptor ligation and clustering mediates signaling via immune receptor tyrosine-based activation motifs (ITAM) on the cytosolic tail of the receptors (Sanchez-Mejorada and Rosales, 1998). The ITAM motifs recruit Syk and Src family kinases, leading to downstream activation of PI3 kinases and Rho family GTPases (mainly Rac1 and Cdc42) to drive both actin polymerization and membrane extension (Vidarsson and van de Winkel, 1998; Cox *et al.*, 2000). IgG-coated particles are internalized through a zipper mechanism whereby pseudopods appear to reach out and surround the particle, binding it within a tight phagosome (Tjelle *et al.*, 2000).

By comparison, complement receptor 3 (CR3 also known as the integrin CD11b/CD18 or Mac-1) requires an additional activation signal for efficient particle binding and phagocytosis. Activation signals can be provided by a number of stimuli such as phorbol esters, lipopolysaccharides (LPS), cytokines, growth factors, and chemokines, which activate protein kinase C (PKC) and induce "inside-out" signaling to integrin receptors (Wright and Silverstein, 1982; Griffin and Mullinax, 1985; Ross and Vetvicka, 1993; Williams and Solomkin, 1999; Schmidt *et al.*, 2001). This signal is translated to changes in integrin tertiary structure and clustering, which enhances receptor affinity and valency (Wright and Griffin, 1985; Hughes and Pfaff, 1998; van Kooyk and Figdor, 2000). Studies on the mechanism of C3bi-particle binding in macrophages have focused primarily on signaling events upstream of Mac-1 activation, with less emphasis on plasma membrane remodeling events. Instead, there has been a concentrated effort to elucidate the underlying mechanisms of C3bi-particle internalization. Binding and clustering of Mac-1 by complement-opsonized particles induces serine phosphorylation of the receptor, which activates the

This article was published online ahead of print in *MBC in Press* (http://www.molbiolcell.org/cgi/doi/10.1091/mbc.E08–02–0223) on September 3, 2008.

Address correspondence to: Rene E. Harrison (harrison@utsc.utoronto.ca).

Abbreviations used: DIC, differential interference contrast; LPS, lipopolysaccharide; MT, microtubule; MTOC, microtubule organizing centre; PMA, phorbol 12-myristate 12-acetate; SEM, scanning electron microscopy; sRBC, sheep red blood cell; TIRFM, total internal reflection fluorescence microscopy.

© 2008 by The American Society for Cell Biology

RhoA GTPase. Activated RhoA signals to serine/threonine kinases to mobilize Arp2/3 and actomyosin-based machinery leading to a slow contractile sinking of the particle into the cytoplasm (Caron and Hall, 1998; Olazabal *et al.*, 2002). Although clarifying the role of actin in Mac-1–mediated phagocytosis has been the subject of intensive research in recent years, much less is known about the role of microtubules (MTs) in this process (Newman *et al.*, 1991; Allen and Aderem, 1996).

In addition to the aforementioned findings, several studies have identified other differences in signaling and cytoskeletal proteins recruited to bound IgG- versus C3bi-opsonized particles (reviewed in Cox *et al.*, 2000). Notably, it has been widely believed that Mac-1–mediated phagocytosis occurs in the absence of the plasma membrane extensions that are a hallmark feature of FcγR-mediated phagocytosis (Kaplan, 1977; Allen and Aderem, 1996; Aderem and Underhill, 1999). Recently however, prominent membrane extensions were observed at the site of C3bi-particle binding (Hall *et al.*, 2006). Here, we reexamine the plasma membrane requirements for Mac-1–mediated phagocytosis using scanning electron microscopy and imaged active membrane protrusions during C3bi-binding utilizing differential interference contrast (DIC) imaging of live cells. Mac-1 receptor display was quantified in control and activated macrophages using flow cytometry. Using a combination of fluorescent microscopy as well as total internal reflection fluorescence (TIRF) imaging during "frustrated phagocytosis," we characterize the major cytoskeletal and intracellular membrane contributors to C3bi-particle binding. Collectively, our analyses provide new insight into the mechanism of Mac-1–mediated phagocytosis in activated macrophages and define a novel role for macropinocytosis in this process.

MATERIALS AND METHODS

Reagents and Antibodies

DMEM, fetal bovine serum (FBS), RPMI 1640, and RPMI 1640 containing 25 mM HEPES (HPMI) were purchased from Wisent (Quebec, QC, Canada). Sheep red blood cells (sRBCs) and rabbit anti-sRBC immunoglobulin M (IgM) were obtained from MP Biomedicals (Solon, OH) and RDI (Research Diagnostics, Concord, MA), respectively. Antibodies were obtained as follows: mouse monoclonal anti-talin, anti-actin, and anti-α-tubulin were from Sigma (St. Louis, MO). Rat anti-mouse CD11b (M1/70) mAb was from AbD Serotec (Oxford, United Kingdom). mAb CBRM1/5 (anti-human CD11b) was purchased from eBioscience (San Diego, CA). Rat IgG2b mAb was from BD PharMingen (San Jose, CA). All fluorescently labeled secondary antibodies were purchased from Jackson ImmunoResearch Laboratories (West Grove, PA). 4′-6-Diamidino-2-phenylindole (DAPI), rhodamine-phalloidin, Oregon green 488-phalloidin and Lucifer yellow CH dilithium salt (LY) were from Invitrogen Canada (Burlington, ON, Canada). Complement C5-deficient human serum, paclitaxel, phorbol 12-myristate 12-acetate (PMA), Hanks' buffered saline solution (HBSS), nocodazole (Noc), amiloride, 1 M HEPES buffer, and all other reagents were purchased from Sigma-Aldrich.

Cell Culture and Transfection

The RAW264.7 macrophage cell line was obtained from the American Type Culture Collection (Rockville, MD) and maintained at 37°C supplied with 5% CO_2 in DMEM supplemented with 10% heat-inactivated FBS. U937 human monocyte cells (American Type Culture Collection, Manassas, VA) were grown in suspension cultures in RPMI 1640 medium supplemented with 10% heat-inactivated FBS at standard cell culture conditions (37°C, humidified 5% CO_2 in air). To induce differentiation, U937 cells were seeded onto glass coverslips supplemented with 1 ml of medium containing 10 nM PMA. After 24 h, nonadhered cells were washed off and cells were grown in RPMI 1640 medium with 10% FBS for 24 h to allow the cells to recover from PMA activation.

Human monocyte-derived macrophages were isolated by plating the lymphocyte/monocyte-rich layer of blood from healthy volunteers on coverslips bathed in DMEM with 10% FBS, incubating them at 37°C, followed by washing with sterile PBS and changing the medium daily for 5 d to remove platelets and lymphocytes.

Peritoneal macrophages were prepared from 3-mo-old C57BL/6 mice and 6- to 8-wk-old TLR4$^{-/-}$ C57BL/6 male mice as described (Khandani *et al.*, 2007). All procedures were approved by the University Health Network Animal Care Committee according to the guidelines of the Canadian Council on Animal Care. Resident (control) macrophages were obtained by peritoneal lavage with 5.0 ml of PBS with 5% heat-inactivated FBS. Elicited peritoneal macrophages were harvested 4 d after injection of 0.8 ml of 4% sterile aged (2 mo or more) Brewer's TG broth (Difco Laboratories, Detroit, MI) by lavage with ice-cold PBS (5 ml) containing 5% FBS and penicillin/streptomycin (100 IU/ml penicillin and 100 μg/ml streptomycin). Resident and thioglycollate-elicited macrophages were washed twice in growth medium containing antibiotics and plated onto poly-L-lysine–coated (0.2 mg/ml, overnight) glass coverslips or 13-mm-diameter thermanex plastic coverslips and grown in DMEM supplemented with 10% FBS and antibiotics (100 IU/ml penicillin and 100 μg/ml streptomycin) at 37°C in 5% CO_2 for 2 h before washing away nonadherent cells.

To study vesicle and MT contribution to membrane ruffle formation, RAW264.7 cells plated on glass coverslips were transiently transfected with cDNA for either wild-type (WT) enhanced green fluorescent protein (EGFP)-Rab11 WT, EGFP-Rab11 S25N (dominant negative [DN]), EGFP-Rab5 S34N (DN), EGFP-Rab34 T66N (DN), or EGFP-Kif5B DN using FuGENEHD (Roche Diagnostics, Indianapolis, IN), according to the manufacturer's instructions.

Mac-1–mediated Phagocytosis

C3bi-opsonized sheep RBCs were prepared as previously described (Jongstra-Bilen *et al.*, 2003). For C3bi-sRBC binding assays, serum-starved RAW264.7 cells were stimulated with 150 nM PMA (15 min) or 10 μg/ml LPS (6 h) or 10 μM taxol (30 min). Where indicated, activated cells were pretreated with 5 mM amiloride (30 min), 2 μM cytochalasin D (20 min), 10 μM Noc (20 min) or were incubated with 5 μg/ml Mac-1 blocking antibody (M1/70) in the presence of 1% FCS. For Noc washout experiments, cells were washed twice with PBS after a 10 μM Noc treatment (20 min) and were further incubated with 150 nM PMA (15 min). After treatments, C3bi-sRBCs were then incubated with macrophages for 12 min to allow binding. Drugs were maintained throughout the period of C3bi-sRBC binding.

Immunofluorescence and Epifluorescence/Confocal Microscopy

After experimental assays, macrophages were washed with PBS and fixed and immunostained as described (Khandani *et al.*, 2007). The primary antibody dilutions used were as follows: Mac-1 (1:1000), talin (1:2000), and α-tubulin (1:10,000). Actin was stained with Oregon Green 488 phalloidin (1:500) or mouse monoclonal anti-β-actin antibody (1:1000). For talin/actin costaining, cells were first incubated with talin then a Cy3-labeled secondary antibody, followed by an additional blocking step before actin immunostaining. All cells were stained with DAPI before mounting, and images were taken with a Zeiss LSM 510 laser scanning confocal microscope or a Zeiss Axiovert 200M microscope equipped with DIC and epifluorescence optics (Carl Zeiss Microimaging, Jena, Germany).

For CLIP-170 immunostaining, cells were fixed in cold methanol containing 1 mM EGTA at −20°C for 10 min, followed by 15 min in 4% paraformaldehyde (PF)/PBS at room temperature, to preserve MT plus ends (Coquelle *et al.*, 2002). Cells were permeabilized with 0.15% Triton X-100/PBS for 20 min and then blocked in 1% BSA/PBS before a 1-h incubation with the polyclonal CLIP-170 antibody. Where indicated cells were also stained with a monoclonal GFP antibody (Abcam, Cambridge, MA) or actin Abs. After staining with fluorochrome-conjugated secondary Abs, coverslips were placed in Attofluor chambers filled with PBS, and cells were then visualized using TIRF laser.

Mac-1 activation in membrane ruffles was monitored using a CBRM1/5 mAb, which detects a conformational change in CD11b within the high-affinity state of Mac-1 (Diamond and Springer, 1993). Differentiated U937 cell without or with PMA stimulation (150 nM for 15 min) at 37°C were incubated with CBRM1/5 mAbs for 10 min at 37°C. Cells were washed with ice-cold PBS and promptly transferred to 4°C and incubated with Cy3-labeled secondary antibody prepared in cold 1% BSA/PBS for 20 min. Cells were fixed with 4% PF/PBS for 20 min on ice. Fixed cells were blocked before F-actin staining with Oregon Green 488 phalloidin. All cells were mounted and images were taken with a Zeiss LSM 510 laser scanning confocal microscope.

Live Imaging of Membrane Ruffles and Mac-1–mediated Phagocytosis

For time-lapse imaging of live macrophages, nontransfected and EGFP-Rab11 WT, EGFP-Rab11 DN, EGFP-Rab5 DN, and EGFP-Rab34 DN-transfected RAW264.7 cells were grown on glass coverslips. Control or activated cells were placed in an Attofluor chamber filled with HPMI and mounted in a temperature-controlled stage heater set at 37°C on an inverted microscope. DIC and epifluorescence images were acquired without or with C3bi-opsonized sRBCs for a period of ~25 min at 10-s intervals using a Zeiss inverted microscope (Axiovert 200 M). In some instances, PMA- and LPS-treated cells were exposed to 0.5 mg/ml LY in the presence of C3bi-sRBCs for 12 min at 37°C. Cells were washed and viewed live by DIC and epifluorescence mi-

croscopy. A similar procedure was followed for live imaging of resident macrophages and TLR4$^{-/-}$ mouse macrophages with or without stimulation by different concentrations of LPS (10 μg/ml, 100 ng/ml, and 10 ng/ml for 6 h).

Flow Cytometry

To analyze cell surface expression of Mac-1, surface immunolabeling with the rat anti-mouse CD11b (M1/70) was performed. Briefly, cells were prestimulated with 150 nM PMA or 10 μg/ml LPS. Where indicated, cells were pretreated with 10 μM Noc in the presence of PMA/LPS or with 10 μM taxol alone. For flow cytometry, 2–5 $\times$ 10^5 cells were collected and washed twice with ice-cold HBSS containing 10 mM HEPES, pH 7.0, 0.02% sodium azide, and 1% FCS (HHF) before blocking with 5% FCS for 15 min. Cells were stained with 1 μg/ml primary antibodies (rat anti-mouse CD11b (M1/70) or rat IgG2b isotype control) for 30 min on ice. After washing twice with HHF, cells were incubated for 30 min on ice with 1 μg PE-conjugated f(ab')2 fragments of anti-rat IgG secondary antibody. Cells were washed twice and resuspended in 500 μl HHF buffer and analyzed for surface staining of Mac-1 or isotype control with FACS-Calibur (Becton Dickinson, San Diego, CA) and CellQuest Software (BD Biosciences, San Jose, CA). The total populations of viable cells were gated to their forward and side scatter. Control samples were evaluated in each experiment. The fluorescence of untreated cells was recorded to determine the level of background fluorescence for negative control cells, whereas treated cells with primary and secondary antibody staining were used as positive control cells. A total of 10,000 event files for each sample were acquired individually in "live-gate" mode. The results were expressed as relative fluorescence intensity (RFI) calculated as geometric mean fluorescence intensity (GFI) of stimulated cells/GFI of control (unstimulated) cells. The experiment was repeated three times and the expression levels were expressed as the mean $\pm$ SEM. Statistical significance was determined using the Student's *t* test.

Mac-1–mediated "Frustrated Phagocytosis" Assay and TIRF Microscopy

Untreated RAW264.7 cells and those transfected with EGFP-Rab11 were scraped and centrifuged at 1000 rpm for 5 min. Cells were then resuspended and rotated in HPMI for 3 h at room temperature to allow receptor recovery. Cells in suspension were prestimulated with PMA or LPS, with and without cytoskeletal disrupting drugs, as described above, or left unstimulated (control). The C3bi-coated coverslips were prepared by coating the glass coverslips with IgM for 1 h at room temperature followed by coating with C5-deficient human serum diluted in PBS (with 1 mM $MgCl_2$, 1 mM $CaCl_2$), for 20 min at 37°C. Cells were plated onto C3bi-coated coverslips to induce frustrated phagocytosis and processed for immunofluorescence. For frustrated phagocytosis control experiments, PMA-stimulated cells were plated onto glass-, BSA (1 mg/ml for 1 h)-, or IgM alone–coated coverslips for 25 min. Cells were fixed and stained for F-actin using Oregon Green 488 phalloidin followed by epifluorescence microscopy.

For dual-color TIRF imaging (see Figures 5E and 6A), cells were fixed after frustrated phagocytosis assays and stained using standard immunofluorescence procedures, as described previously. Coverslips were placed in Attofluor chambers filled with PBS. A TIRF multilane argon-ion laser was used for excitation of both GFP and Cy3 (excitation λ = 488 nm and excitation λ = 514, 100 mW, respectively).

Scanning Electron Microscopy

Primary human monocyte-derived macrophages, resident mouse macrophages, thioglycollate-elicited mouse macrophages, and RAW264.7 cells grown on plastic thermanex coverslips were serum-starved for 3 h. Where indicated, cells were prestimulated with 150 nM PMA or 10 μg/ml LPS or 10 μM taxol, with and without cytoskeletal disrupting drugs, as described above, or left unstimulated (control). Cells were then incubated with or without C3bi-sRBCs for 12 min to allow binding. After incubation, cells were rinsed with PBS and processed for scanning electron microscopy (SEM) as described (Khandani *et al.*, 2007). Electron micrographs were pseudocolored using Adobe Photoshop 7.0 (San Jose, CA).

Quantification and Statistics

For determination of particle binding index, the number of C3bi-sRBCs or unopsonized sRBCs bound per 100 macrophage cells were tabulated in PMA- and LPS-activated macrophages, thioglycollate-elicited macrophage, as well as for cells treated with amiloride or Mac-1 blocking antibodies. For immunofluorescence experiments, quantification was performed by calculating the number of bound C3bi-sRBCs per 100 macrophages. The number of C3bi-sRBCs associated with ruffles containing extended F-actin networks per 100 macrophages was determined by visual inspection of immunofluorescence images. C3bi-sRBCs were scored as positively associating with F-actin ruffles when the ruffle was directly apposed to the sRBC and surrounded more than one-third of the particle. When ruffles were at a distance more than one-half a sRBC diameter (~1.5 μm) away from the particle they were not scored as positive. For EGFP-Rab11 WT, EGFP-Rab11 DN, EGFP-Rab5 DN, and EGFP-Rab34 DN transfection experiments, the number of total bound C3bi-sRBCs and C3bi-sRBCs associated with actin ruffles in 50 transfected cells were counted for both stimulated and nonstimulated cells. For "frustrated phagocytosis" quantification, the number of macrophages adhered to the glass-, BSA-, IgM-, and C3bi-coated coverslips were counted for each treatment. A minimum of three replicates per condition was performed (n >20).

To analyze the cell area of adhered cells during frustrated phagocytosis, digitized images of phalloidin stained cells were acquired by epifluorescence microscopy and analyzed with Image J (http://rsb.info.nih.gov/ij/; NIH, Bethesda, MD). Relative increase in cell size was calculated by dividing the mean size of cells plated on BSA-, IgM-, or C3bi-coated coverslips by the mean size of cells plated on glass coverslips. All statistical analyses were performed using the Student's *t* test. Error bars represented in graphs denote the SEM. Data presented are from at least three representative experiments.

RESULTS

Membrane Ruffles Are Associated with Bound C3bi-sRBCs

It is widely believed that Mac-1–mediated phagocytosis involves "sinking" of C3bi particles without contributions of membrane pseudopods that have been well-characterized in FcγR-mediated phagocytosis (Kaplan, 1977; Allen and Aderem, 1996; Aderem and Underhill, 1999). We reexamined the plasma membrane surface topology during Mac-1–mediated phagocytosis using SEM. To activate integrins, RAW264.7 cells, mouse resident peritoneal macrophages and human monocyte-derived macrophages were treated with the phorbol ester, PMA (150 nM for 15 min), a common approach for integrin activation (Allen and Aderem, 1996; Lim *et al.*, 2007), before 12-min exposure to C3bi-sRBCs. Surprisingly, our SEM analysis revealed large membrane ruffles on the dorsal surface of the macrophages that consistently associated with C3bi-sRBCs (Figure 1). Unlike pseudopods formed during FcγR-mediated phagocytosis, which tightly associate around the circumference of the particle, the ruffles were often on one side of the C3bi-sRBCs appearing as a "wave" extending over the particle. The C3bi-sRBCs were more frequently associated with the ruffles than with flat, quiescent regions of the plasma membrane. In contrast, untreated control cells showed very few membrane ruffles and negligible binding to C3bi-sRBCs (Figure 1). To see if this was a general phenomenon in activated macrophages, we also performed SEM analysis of C3bi-sRBC binding in macrophages activated with the bacterial cell wall product, LPS (10 μg/ml, 6 h). SEM analysis again revealed broad ruffles with which C3bi-sRBCs were associated (Figure 1) in both mouse and human monocyte-derived macrophages.

Dorsal ruffles were induced by PMA and LPS in the absence of C3bi particles (Figure 1 and Swanson, 1989; Williams and Ridley, 2000), indicating that membrane ruffles are not induced by C3bi-particle outside-in signaling, but rather that C3bi particles preferentially associate with preexisting ruffles. Because higher doses of LPS can affect cellular membranes (Bannerman and Goldblum, 1999), we further examined a range of LPS concentrations on membrane ruffling. Lower concentrations of LPS (100 ng/ml for 6 h) showed membrane ruffle formation and association of ruffles with C3bi-sRBCs, using DIC imaging and phalloidin staining and immunofluorescence, respectively (see Supplementary Figures S1C and S2). Ruffle formation and C3bi-sRBC particle association were not present in unstimulated resident macrophages or those stimulated with 10 ng/ml LPS for 6 h (Supplementary Figures S1D and S2). LPS did not induce membrane ruffles or C3bi-sRBC binding even at the highest concentrations in peritoneal macrophages from TLR4 knockout (−/−) mice (Supplementary Figures 1 and 2), indicating that LPS-induced membrane ruffles were generated through TLR4 signaling.

To investigate whether membrane ruffling and C3bi particle capture occurs in macrophages stimulated in vivo, thio-

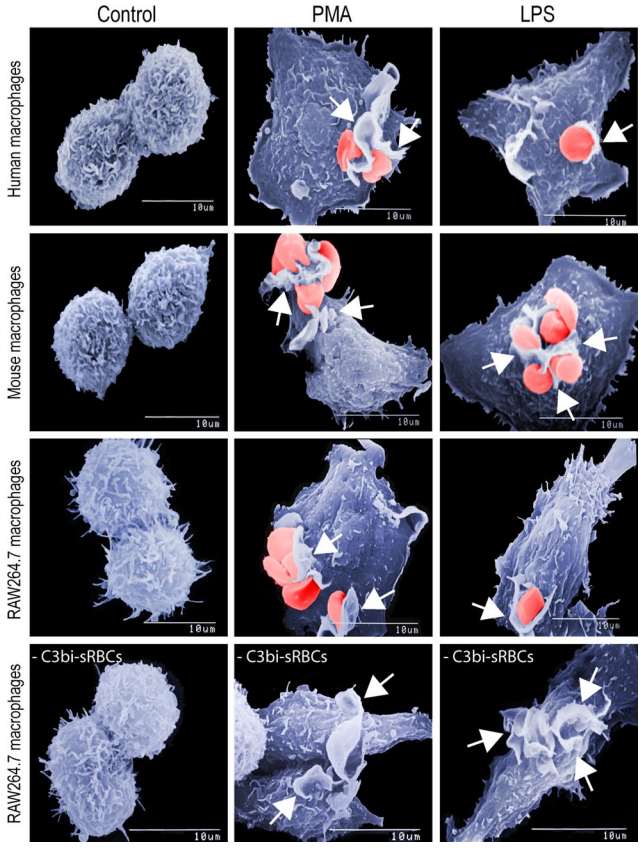

Figure 1. PMA- or LPS-induced membrane ruffles are associated with C3bi-sRBCs. RAW264.7 mouse macrophages, primary mouse peritoneal macrophages and human monocyte-derived macrophages were isolated and plated as described in *Materials and Methods*. Macrophages were serum-starved for 3 h before activation with 150 nM PMA for 15 min or 10 μg/ml LPS for 6 h. Cells were exposed to C3bi-sRBCs for 12 min, or directly fixed after activation, before processing for SEM. No visible membrane ruffles or bound C3bi-sRBCs were observed in unstimulated (control) macrophages. In contrast, PMA- and LPS-activated macrophages exhibited broad dorsal ruffles that partially surrounded bound C3bi-sRBCs (arrows). In the absence of C3bi-sRBCs, PMA-, and LPS-stimulated macrophages showed pronounced membrane ruffles, which are lacking in control, unstimulated RAW264.7 cells. Scale bars, 10 μm.

glycollate-elicited mouse peritoneal macrophages were examined. Thioglycollate-elicited macrophage also showed membrane ruffles engaging C3bi-sRBCS both by SEM analysis and epifluorescence of phalloidin and C3bi-sRBC stained samples, which were absent from resident peritoneal macrophages (Supplementary Figure S3, A and B). Collectively, these results implicate membrane ruffles in particle adherence during Mac-1–mediated phagocytosis.

Macropinocytosis Membrane Ruffles Are Involved in C3bi-sRBC Binding

We next turned to live DIC imaging of macrophages to more fully understand the interrelationship between surface membrane ruffles and C3bi-particle binding. DIC images were captured at 10-s intervals shortly after particle addition in both PMA- and LPS-activated RAW264.7 cells. Live imaging revealed prominent membrane ruffles that formed spontaneously on the dorsal surface of activated, but not on control cells (Figure 2 A, also see Supplementary Movie S2A, control). Excess C3bi-sRBCs were added, and particles that encountered broad regions of ruffles showed preferential binding to these surfaces, compared with inactive membrane regions (Figure 2A, see Supplementary Movie S2A, PMA). C3bi-sRBCs that only made slight contact with ruffles were stalled but not captured. In comparison, C3bi-sRBCs that made full contact with ruffles were stopped, after which the C3bi-sRBCs were pulled toward the macrophage cell body as the ruffle collapsed toward the cell membrane (Figure 2A, see Supplementary Movie S2A, PMA). Similar to our SEM results, ruffles were often associated with one side of the particle (Figure 2A). After adherence of the particle to the macrophage cell surface, we frequently observed large vesicles appearing in the cytoplasm beneath the bound particle (Figure 2A, see Supplementary Movie S2A, PMA).

Dorsal ruffles on macrophages are frequently associated with macropinocytosis (Racoosin and Swanson, 1992). Moreover, we often observed empty vesicles forming beneath bound particles that may represent macropinosomes. To verify that the C3bi-particle–associated ruffles were macropinocytosis ruffles we exposed cells to C3bi-sRBCs for 12 min in DMEM containing 0.5 mg/ml Lucifer Yellow (LY), to label macropinosomes (Racoosin and Swanson, 1992). The cells were washed and the intracellular distribution of LY was followed using fluorescence microscopy in both stimulated (PMA or LPS) and resting RAW264.7 cells. In nonstimulated cells, very few cells contained LY-positive vacuoles and minimal C3bi-sRBC binding was observed (Figure 2B). However, in PMA- and LPS-activated macrophages, many LY-labeled vesicles were observed beneath the bound particles (Figure 2B). To corroborate the notion that macropinocytosis and Mac-1–mediated phagocytosis were linked, we treated cells with amiloride, a potent inhibitor of membrane ruffling and macropinocytosis (Dowrick *et al.*, 1993; Swanson and Watts, 1995). Amiloride treatment blocked both ruffle formation and LY uptake in both PMA- and LPS-treated RAW264.7 cells (not shown). PMA-stimulated cells, pretreated with amiloride, had dramatically reduced bound C3bi-sRBCs, to levels observed in unstimulated macrophages (Figure 2C).

To test whether membrane ruffles could independently capture sRBCs, unopsonized particles were added to PMA-activated macrophages and after 12 min, cells were washed and fixed, and bound particles were tabulated. Bound, unopsonized sRBCs were virtually absent on activated macrophages (Figure 2C). When Mac-1–blocking antibodies were added to the media, ruffles formed normally in PMA-stimulated macrophages (not shown), but C3bi-sRBC binding abilities were abolished in these cells (Figure 2C).

Membrane Ruffles Are Enriched in Mac-1 and Talin

Why might C3bi particles selectively associate with membrane ruffles? Our live DIC imaging results suggest that membrane ruffles assist in C3bi-sRBCs adherence to the macrophage cell surface. However, ruffles were not sufficient to capture unopsonized particles (Figure 2C), showing a necessity for Mac-1 in C3bi-sRBC binding. We examined Mac-1 distribution in PMA- and LPS-stimulated RAW264.7 cells exposed to C3bi-sRBCs for 12 min. As shown in Figure 3A, Mac-1 was enriched in actin-dense protrusions that were identified as membrane ruffles by DIC imaging. Mac-1 was also observed in membrane ruffles not engaged in particle binding (Figure 3A). To determine the mechanism for enhanced Mac-1 recruitment within membrane ruffles, we next examined the distribution of talin during C3bi-particle binding in macrophages. Talin is a cytoskeletal protein that binds to integrin β cytoplasmic domains and is a critical regulator of integrin clustering and affinity (Ratnikov *et al.*, 2005; Simonson *et al.*, 2006; Lim *et al.*, 2007). Importantly, talin is

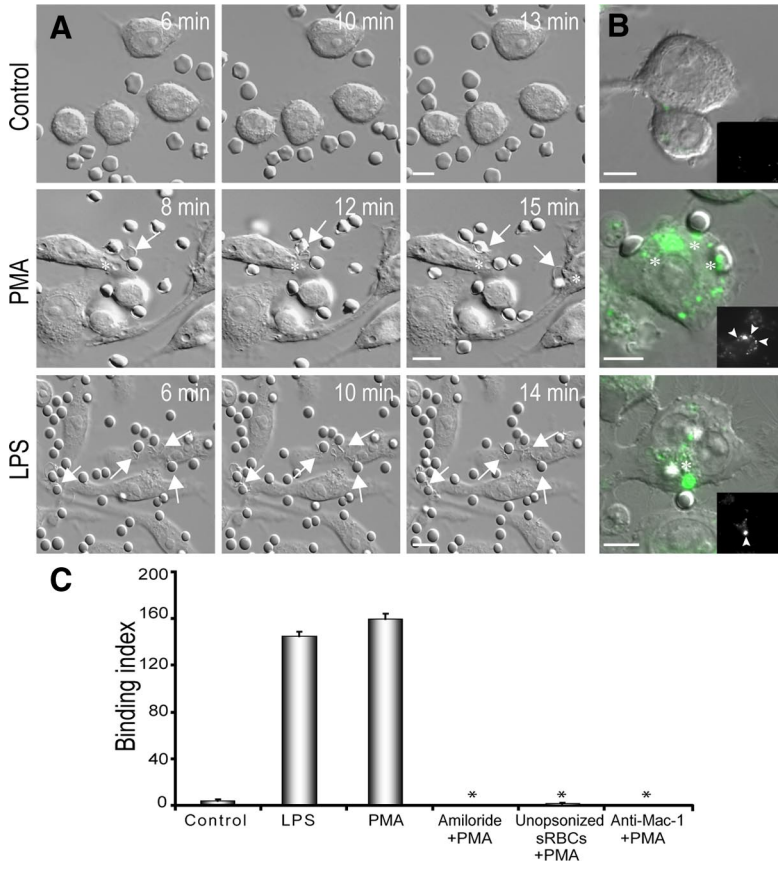

Figure 2. Membrane ruffles mediate capture of C3bi-sRBCs. (A) Selected stills from DIC time-lapse movies of serum-starved control RAW264.7 cells and cells stimulated with 150 nM PMA for 15 min or 10 μg/ml LPS for 6 h. Imaging began after addition of C3bi-sRBCs. Ruffle formation was not observed in control cells and C3bi-sRBCs drifted past the cells without binding (see also Supplementary Movie S2A control). In contrast, PMA- and LPS-stimulated macrophages showed prominent membrane ruffles (arrows), which contacted approaching C3bi-sRBCs (white arrow, Supplementary Movie S2A, PMA). After ruffle contact with C3bi-sRBCs, particles were pulled toward the macrophage cell body as the ruffle collapsed. Appearance of large empty vesicles occurred beneath the initial site of ruffle contact with C3bi-sRBCs (asterisks). (B) Control, PMA-, and LPS-activated RAW264.7 cells were exposed to C3bi-sRBCs in the presence of Lucifer Yellow, a fluorescent indicator of macropinosomes. Epifluorescent and DIC overlay images revealed the accumulation of Lucifer yellow (asterisks) beneath bound C3bi-sRBCs. The corresponding epifluorescence images are shown in insets. Arrowheads mark the site of bound particle. Scale bars, 10 μm. (C) Determination of binding index representing the number of C3bi-sRBCs or unopsonized sRBCs bound per 100 RAW264.7 macrophages treated with or without 150 nM PMA (15 min) or 10 μg/ml LPS (6 h) or PMA + 5 mM amiloride (30 min) or PMA + 5 μg/ml Mac-1–blocking antibody (M1/70). * $p < 0.05$ compared with the PMA alone-stimulated cells ($n > 20$). Data represents mean and SEM from three separate experiments.

enriched at sites of C3bi-particle binding (Allen and Aderem, 1996) and is essential for C3bi-particle binding and phagocytosis (Lim *et al.*, 2007). Immunostaining for talin and actin revealed a strong colocalization of these proteins in membrane ruffles alone or those containing C3bi-sRBCs (Figure 3B). To directly assess whether Mac-1 was activated within membrane ruffles, we examined the integrin activation state using the CBRM1/5 antibody. CBRM1/5 is a mAb that recognizes an activation epitope on a subset of CD11b molecules on macrophages only after the integrin undergoes the conformational change associated with activation (Diamond and Springer, 1993). Because the conformation-sensitive mAb does not recognize murine integrins, we used the human monocytic U937 cell line for these experiments. Stimulation of cells with PMA induced the expression enriched staining of CBRM1/5 at F-actin–rich membrane ruffles in differentiated U937 cells (Figure 3D) compared with the unstimulated control cells (Figure 3C). The presence of activated Mac-1 and talin in membrane ruffles further suggests an adherence role for membrane ruffles during Mac-1–mediated phagocytosis.

Macrophage Activation Increases Mac-1 Surface Expression

Neutrophils up-regulate surface integrin expression after PMA stimulation (Sengelov, 1995). We investigated whether macrophage activation promoted Mac-1 delivery to the plasma membrane using flow cytometry. Treatment of RAW264.7 cells with PMA caused an increase in surface Mac-1 compared with control (untreated) cells and cells stained with the isotype control (Figure 4, A and F). LPS stimulation also enhanced surface Mac-1 expression, compared with untreated cells (Figure 4, B and F). Immunofluorescent analysis revealed that the bulk of Mac-1 was concentrated in membrane ruffles in PMA- and LPS-activated macrophages (Figure 4, A and B). Because targeted delivery of intracellular components often requires the MT cytoskeleton, we treated activated macrophages with Noc, before surface staining for Mac-1. Noc treatment blunted surface expression of Mac-1 in both PMA- and LPS-stimulated macrophages (Figure 4, C, D, and F). Studies on macrophages have shown that PMA stimulates MT assembly and LPS promotes MT stabilization (Phaire-Washington *et al.*, 1980; Binker *et al.*, 2007). We next queried whether MT stabilization alone could promote delivery of integrins to the cell surface, by treating cells with taxol. Taxol stimulation of RAW264.7 cells induced integrin clustering in membrane ruffles but did not substantially influence the total surface expression of Mac-1, compared with untreated cells (Figure 4, E and F).

Intact Microtubules and Kinesin Are Required for Membrane Ruffle Formation/C3bi-sRBC Adherence

We continued our cytoskeletal analysis by examining the spatial distribution of MTs in membrane ruffles and its functional requirement for Mac-1–mediated phagocytosis. Using immunofluorescence with an anti-α-tubulin antibody and phalloidin staining, we visualized the MT and actin cytoskeletons during membrane ruffle formation/C3bi-sRBC binding. F-actin was enriched in PMA- and LPS-induced membrane ruffles as elongated waves extending perpendicularly from the cell membrane (Figure 5A). These actin extensions were within membrane ruffles identified using DIC and were frequently associated with bound C3bi-sRBCs

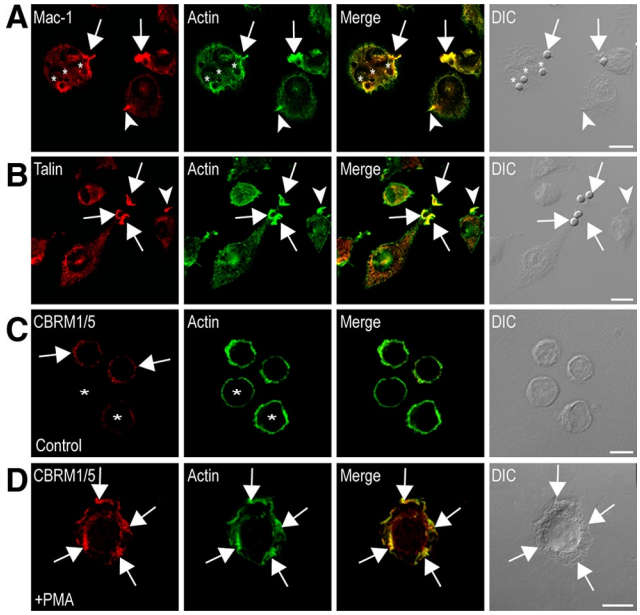

Figure 3. Mac-1 and talin localize to actin-rich membrane ruffles engaged in Mac-1–mediated phagocytosis. RAW264.7 macrophages stimulated with 10 μg/ml LPS were exposed to C3bi-sRBCs and immunostained for (A) Mac-1 (red) and actin (green) or (B) talin (red) and actin (green) as described in *Materials and Methods* and imaged using confocal microscopy. Merged confocal and corresponding DIC images are also shown. Arrows in (A) indicate clustering of Mac-1 into actin-rich membrane ruffles, adjacent to the site of particle attachment. Circular Mac-1 and actin colocalization was also visualized around recently internalized particles (asterisks). Arrows in B illustrate prominent talin and actin colocalization at membrane ruffles surrounding bound C3bi-sRBCs. Arrowheads indicate Mac-1/talin staining enrichment in membrane ruffles not containing C3bi particles. Differentiated U937 cells stimulated without (C) or with 150 nM PMA (15 min; D) were immunostained for activation-specific Mac-1 epitope using CBRM1/5 (red) and actin (green), as described in *Materials and Methods,* and imaged using confocal microscopy. Merged confocal and corresponding DIC images are also shown. (C) Asterisks indicates cells with negligible CBRM1/5 antibody staining; arrows indicate punctate staining at random sites on the cell periphery. (D) Arrows indicate the high-affinity integrin enrichment in actin-containing membrane ruffles in PMA-stimulated cells. Scale bars, 10 μm.

in PMA-, LPS-, and thioglycollate-elicited macrophages (Figure 5A, Supplementary Figure S3B). The number of F-actin–containing ruffles associated with bound particles was quantified (Figure 5C, Supplementary Figure S3C). Cytochalasin D (cyto D)-pretreatment markedly reduced F-actin extension, ruffle formation, and particle binding (Figure 5C). MTs were frequently observed penetrating the sites of F-actin–rich ruffle formation/C3bi-particle contact in both PMA- and LPS- stimulated macrophages (Figure 5A). To depolymerize MTs, Noc was added at the time of PMA stimulation. SEM analysis showed a near complete absence of C3bi-particle binding in Noc-treated cells, and no ruffles were observed by SEM (Figure 5B), similar to cyto D–treated cells (Figure 5B). Quantification of immunofluorescence images showed a near complete absence of bound particles and particles associated with ruffles in Noc-treated cells (Figure 5C). In Noc washout experiments, both ruffle formation and C3bi-sRBC binding was restored in activated RAW264.7 cells (Figure 5, B and C). Very similar results were observed with LPS-activated macrophages (not shown). Taxol-stimulated macrophages exhibited membrane ruffles and showed an increase in bound C3bi-sRBCs, compared with untreated control cells (Figure 5, B and C). We also analyzed the necessity of anterograde MT trafficking for ruffle formation by transfecting cells with a dominant negative construct of the conventional kinesin heavy chain (EGFP-Kif5B DN). A pronounced reduction in both ruffle formation and C3bi-particle binding was observed in PMA-stimulated EGFP-Kif5B DN cells, compared with untransfected cells (Figure 5C).

The interrelationship between F-actin and MTs was difficult to resolve with conventional fluorescent imaging. To more precisely visualize the involvement of actin and MTs during Mac-1–mediated phagocytosis, we devised a Mac-1–mediated "frustrated phagocytosis" assay, which we monitored using TIRF imaging. This novel approach allowed visualization of CLIP-170, a MT plus-end–tracking protein, at sites of Mac-1 ligation, which in this case was a C3bi-coated coverslip (see *Materials and Methods* and Figure 5D). PMA- or LPS-activated macrophages showed high adherence and spreading onto C3bi-coated coverslips, and immunofluorescence analysis revealed broad actin protrusions at the periphery of spread cells (Figure 5E and see Supplementary Figure S4A). CLIP-170 was detected in peripheral actin-rich regions by TIRF microscopy (Figure 5E), suggesting MT penetration into F-actin–rich membrane regions of engagement. To differentiate between frustrated phagocytosis and cell spreading, cells were additionally plated on glass- or BSA- or IgM-coated coverslips, and cell area was measured after 25 min, compared with cells coated on C3bi coverslips. There was a dramatic increase in the cell area of PMA-stimulated RAW264.7 cells parachuted onto C3bi-coated coverslips versus glass alone coverslips or coverslips coated with BSA or IgM only (Supplementary Figure S4B). Moreover, the presence of C3bi ligand on coverslip, strongly promoted cell attachment compared with BSA-, IgM-, or uncoated glass coverslips (Supplementary Figure S4C). These results indicate that Mac-1-ligation and signaling is the predominant influence for spreading associated with frustrated phagocytosis and is distinct from nonphagocytic spreading.

Treatment of PMA-activated cells with either cytochalasin D or Noc abolished the ability of cells to attach to complement-coated coverslips (Figure 5F), which strongly correlated with reduced C3bi-sRBCs binding abilities in cytoskeletal-disrupted cells (Figure 5C). Similarly, activated macrophages exposed to a Noc washout treatment showed enhanced adherence to C3bi coverslips (Figure 5F), in agreement with our C3bi-sRBC binding results (Figure 5C). This validates the C3bi-frustrated phagocytosis assay as an effective means to study cortical membrane events during Mac-1–mediated phagocytosis. Taxol pretreatment also enhanced cell attachment to C3bi coverslips as compared with untreated control cells (Figure 5F). Collectively, our observations using epifluorescence and TIRF microscopy indicate that both F-actin and MTs are key structural and functional components of membrane ruffles required for C3bi-particle binding.

Recycling Endosomes Contribute to Membrane Ruffle Formation/C3bi-sRBC Adherence

We observed that MT depolymerization or kinesin inhibition abolishes membrane ruffle formation, suggesting that MTs may deliver intracellular membranes/integrins to sites of ruffle formation. We chose to monitor delivery of Rab11-containing recycling endosomes to membrane ruffles/C3bi particles, as previous studies have shown that Rab11 recruits vesicles to the plasma membrane in a MT-dependent manner (Yoon *et al.*, 2005). To verify that these EGFP-Rab11–

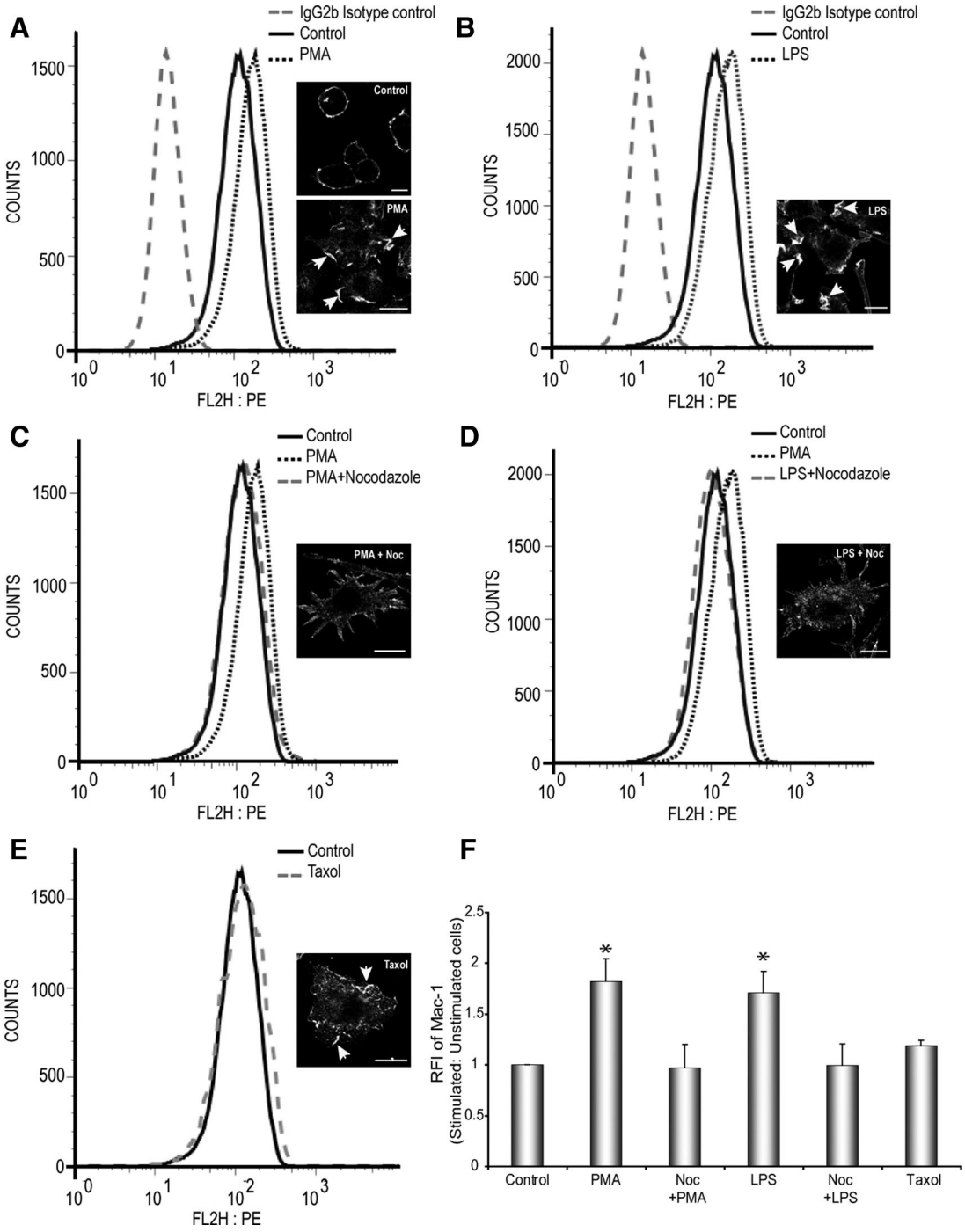

Figure 4. PMA and LPS increase surface Mac-1 expression in a MT-dependent manner. Cell surface expression of Mac-1 in stimulated and unstimulated RAW264.7 macrophages were analyzed by flow cytometry using a mAb against Mac-1. (A and B) Stimulation of RAW264.7 macrophages with 150 nM PMA or 10 μg/ml LPS, respectively, caused an up-regulation of cell surface Mac-1 expression compared with unstimulated cells and cells stained for isotype control. Insets, Mac-1 immunostaining for all conditions; arrows indicate ruffles. Scale bars, 10 μm. (C and D). Pretreatment of Noc in the presence of PMA or LPS inhibits the up-regulation Mac-1 expression on the surface of RAW264.7 cells. (E) Treatment of cells with taxol alone only induces a slight increase in the levels of Mac-1 expression, compared with untreated control cells. (F) Quantitative evaluation of the relative fluorescent intensities (RFI) of stimulated versus unstimulated (control) RAW264.7 macrophages. Data represents mean and SEM from three separate experiments. * $p < 0.05$ compared with control, untreated cells.

positive vesicles accumulated at MT plus ends at sites of cell attachment, EGFP-Rab11 WT was transfected into RAW264.7 cells, and C3bi-frustrated phagocytosis assays were used in LPS-activated cells (Figure 6A). When cells were immunostained for CLIP-170 and GFP and imaged using TIRF microscopy, we observed colocalization of EGFP-Rab11–positive vesicles with CLIP-170 (Figure 6A), suggesting MT-mediated trafficking of Rab11 vesicles to regions of active membrane remodeling. Epifluorescent imaging of an EGFP-Rab11 WT-transfected RAW264.7 cell during

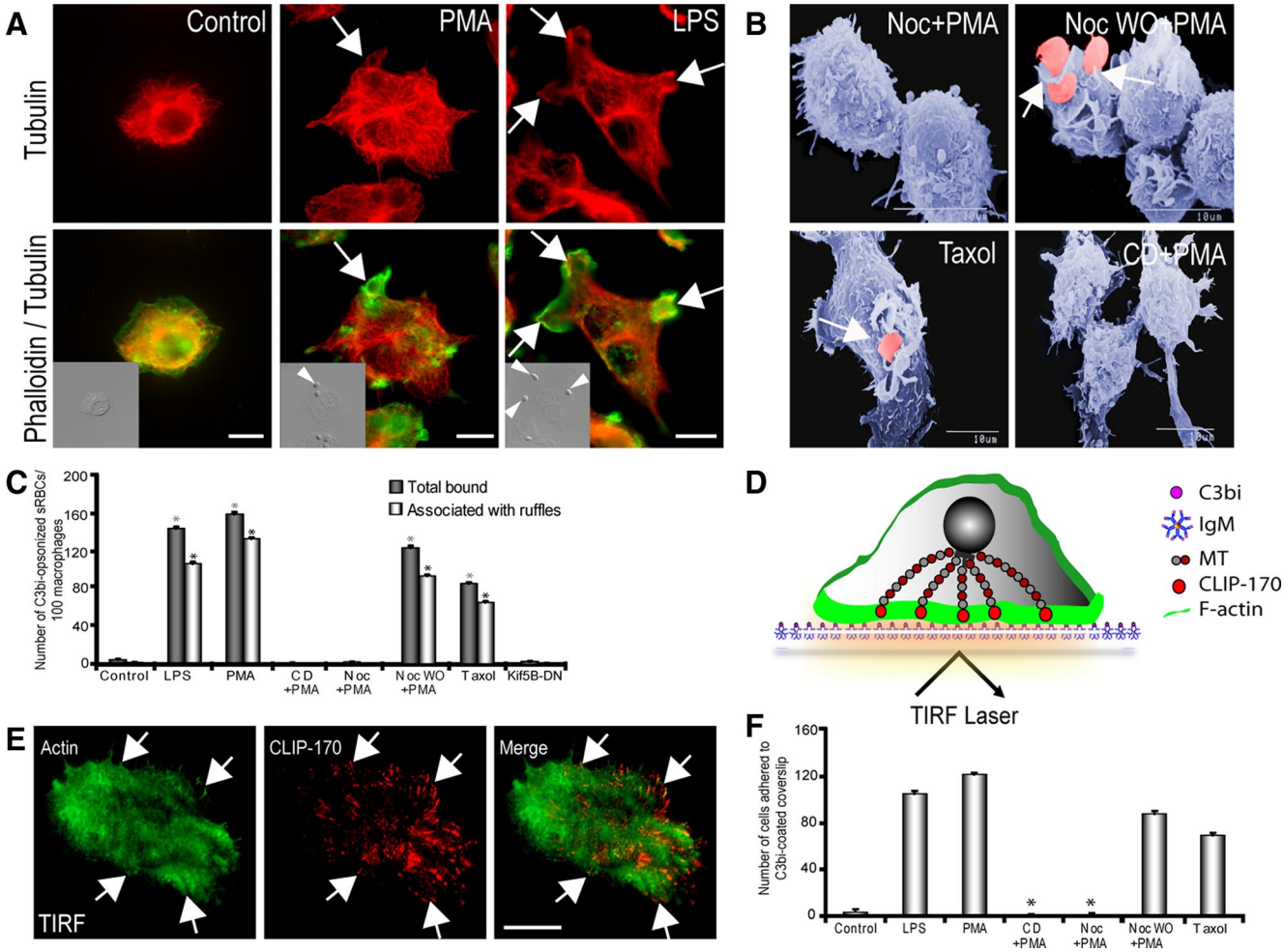

Figure 5. MTs and kinesin are essential for ruffle formation and C3bi-target binding. (A) Immunostaining of MTs and actin in control or PMA- or LPS-stimulated RAW264.7 cells. After C3bi-sRBC binding, cells were fixed and immunostained for α-tubulin (red) and actin (green). Arrows indicate MTs at the site of actin-rich membrane ruffles associated with C3bi-sRBCs. DIC image is shown in insets where C3bi-sRBCs are indicated by arrowheads. (B) Cytoskeletal requirements for ruffle formation and C3bi-sRBC binding was determined by treating cells with nocodazole (Noc) or cytochalasin D (CD) during PMA activation before C3bi-particle binding and SEM processing. Noc treatment inhibited both membrane ruffle formation and particle binding, whereas in Noc washout (Noc WO) experiments, binding of C3bi-sRBCs through membrane ruffles was observed (arrows). Taxol stimulation of macrophages induced ruffles associated with C3bi-sRBCs. Scale bars, 10 μm. (C) Graphic representation of total number of C3bi-sRBCs bound per 100 macrophages and number of bound C3bi-sRBCs associated with membrane ruffles in each treatment (see *Materials and Methods*). Data represents mean and SEM from three separate experiments. * $p < 0.05$ compared with control, untreated macrophages. (D) Cartoon illustration of TIRF microscopy visualization of the actin and MT cytoskeletons during Mac-1–mediated frustrated phagocytosis. (E) RAW264.7 cells serum starved in suspension for 3 h were pretreated with LPS and plated on C3bi-coated coverslips for 25 min. Cells were fixed and immunostained for CLIP-170 (red) and actin (green) and imaged using TIRF microscopy. CLIP-170, which decorates MT plus ends, was observed within peripheral actin-rich protrusions at the cortical regions engaged in phagocytosis (arrows). Scale bar, 10 μm. (F) Quantification of Mac-1–mediated frustrated phagocytosis where the number of RAW264.7 cells adhered to the C3bi-coated coverslips were counted for each treatment. * $p < 0.05$ compared with control, untreated cells. Data are mean and SEM from three separate experiments.

Mac-1–mediated phagocytosis, revealed delivery of EGFP-Rab11 vesicles to a membrane ruffle during the time of C3bi-particle capture, observed using DIC microscopy (Figure 6B, Supplementary Movie S6B, merge). EGFP-Rab11 vesicles moved toward active membrane regions and appeared to cluster along and at the base of ruffles (Figure 6B, Supplementary Movie S6B, GFP). To definitively show Rab11 accumulation at membrane ruffles, cells were fixed and stained for F-actin using phalloidin after particle binding. Enrichment of EGFP-Rab11 WT was observed at the base of F-actin–rich membrane ruffles associated with C3bi particles (Figure 6C).

To determine if Rab11 played a role in integrin recruitment to the plasma membrane, we performed Mac-1 staining and flow cytometry analysis of PMA- and LPS-stimulated RAW264.7 cells transfected with a dominant negative Rab11 construct (EGFP-Rab11 DN). Expression of this construct significantly reduced phagocytosis of IgG-sRBCs compared with untransfected cells (Supplementary Figure S5A), as has been previously described (Cox *et al.*, 2000). When analyzed by flow cytometry, a significant decrease in Mac-1 expression was observed in EGFP-Rab11 DN transfected cells, compared with stimulated untransfected cells (Figure 6D). Expression of an EGFP-Rab11 WT construct did not influence Mac-1 surface expression (not shown). We next looked at whether Rab11 had a role in mediating ruffle formation and C3bi-sRBC binding. Expression of the domi-

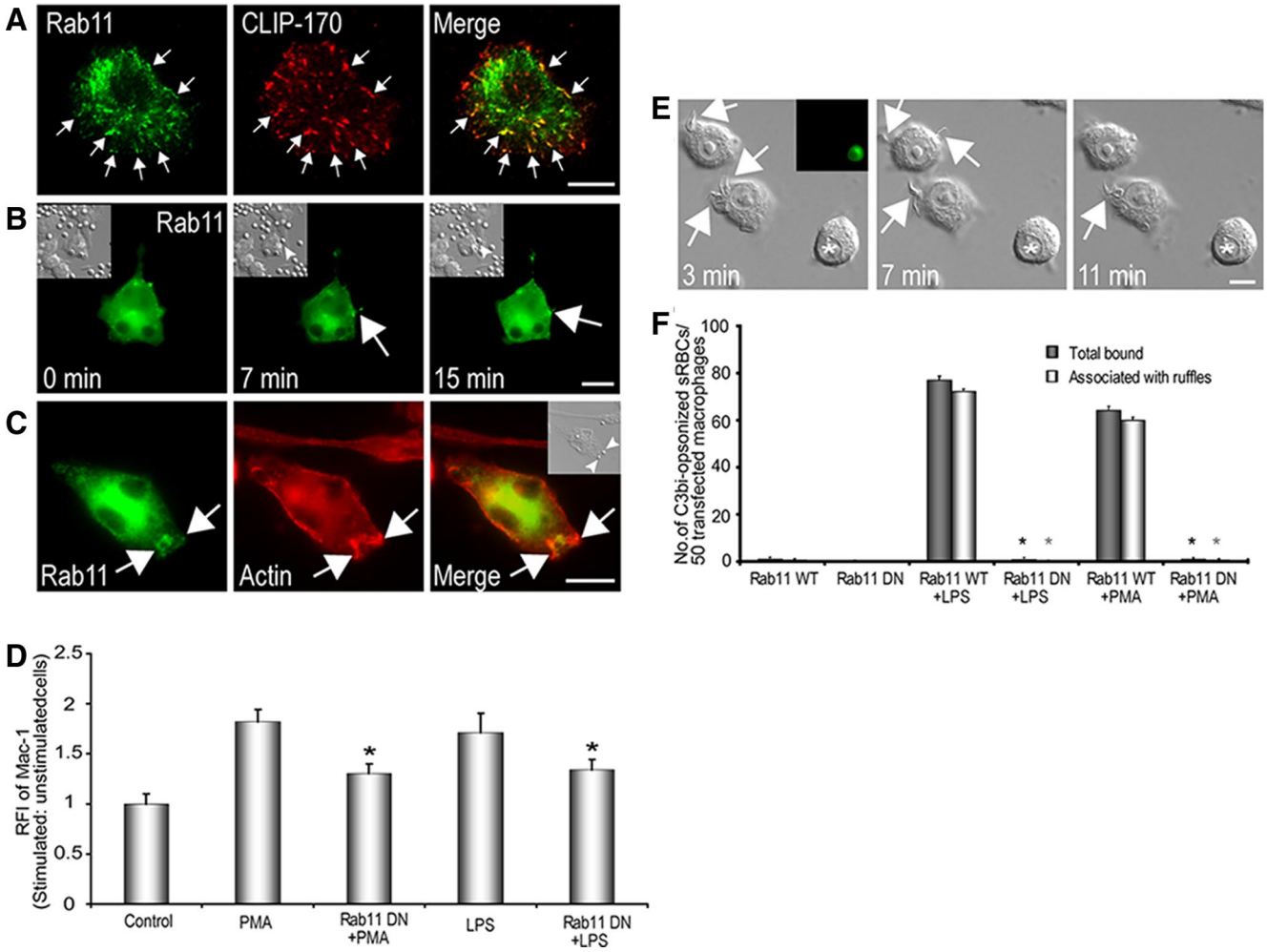

Figure 6. Rab11 requirement for membrane ruffle formation/C3bi-sRBC adherence to macrophages. (A) RAW264.7 cells were transfected with EGFP-Rab11 WT and were activated with 10 μg/ml LPS. Cells were then plated on C3bi-coated coverslips for 25 min, fixed, and immunostained for CLIP-170 (red) and GFP (red). EGFP-Rab11 WT colocalizes with CLIP-170 at MT plus ends (arrows). (B) Representative epifluorescence and corresponding DIC images (insets) of an EGFP-Rab11 WT-transfected RAW264.7 cell stimulated with LPS and exposed to C3bi-sRBCs. EGFP-Rab11 WT-positive vesicles (arrows) can be seen within and at the base of ruffles engaged in C3bi particle capture (arrowhead in DIC images; also see Supplementary Movie S6B, merge, and Supplementary Movie S6B, GFP). Time is indicated in minutes. (C) Epifluorescent image of an EGFP-Rab11 WT transfected cell (green) stained for phalloidin (red). Arrows indicate EGFP-Rab11 WT accumulation at sites of membrane ruffles and bound particles, shown in DIC inset. (D) Relative fluorescent intensity (RFI) of surface Mac-1 in PMA- and LPS-stimulated cells transfected with EGFP-Rab11 DN, compared with stimulated untransfected cells. * $p < 0.05$ compared with LPS- or PMA-stimulated cells. (E) Representative DIC and epifluorescence (inset) images of EGFP-Rab11 DN transfected RAW264.7 cells stimulated with 150 nM PMA. Membrane ruffle formation was reduced by the expression of EGFP-Rab11 DN. Asterisk indicates transfected cell. Ruffling in nontransfected cells is indicated by arrows (see also Supplementary Movie S6E). Scale bars, 10 μm. (F) Quantification of total bound C3bi-sRBCs and number of bound C3bi-sRBCs associated with ruffles per 50 EGFP-Rab11 WT or EGFP-Rab11 DN-transfected cells with or without stimulation with LPS or PMA. Data represents mean and SEM from three separate experiments. * $p < 0.05$ compared with LPS- or PMA-stimulated EGFP-Rab11 WT-transfected cells.

nant negative construct affected membrane ruffle formation in PMA-stimulated RAW264.7 cells compared with neighboring untransfected cells, shown for comparison (Figure 6E, see Supplementary Movie S6E). Whereas some cell surface activity was observed in cells expressing EGFP-Rab11 DN, membrane ruffle extension was severely attenuated. Importantly, overexpression of EGFP-Rab11 DN in PMA- and LPS-activated macrophages dramatically impaired membrane ruffle-mediated C3bi-sRBC binding, compared with cells expressing WT EGFP-Rab11 (Figure 6F). To determine whether Rab11 was the sole Rab responsible for membrane protrusions during ruffle formation, we also examined the requirement for other Rabs implicated in macropinocytosis, namely the early endosomal Rab5 (Li *et al.*, 1997) and Rab34 (Sun *et al.*, 2003). Expression of a dominant negative form of Rab5 did not impact membrane ruffle formation in PMA-stimulated RAW264.7 cells by DIC imaging (Supplementary Figure S5B). C3bi-sRBCs also bound normally to cells expressing Rab5 DN and stimulated with PMA or LPS (Supplementary Figure S5B). Transfection of RAW264.7 cells with Rab34 DN did reduce membrane ruffle formation and C3bi-sRBC binding (Supplementary Figure S5, B and C) implicating Rab34 as well as Rab11 in membrane ruffle-mediated capture of C3bi-opsonized particles during Mac-1–mediated phagocytosis.

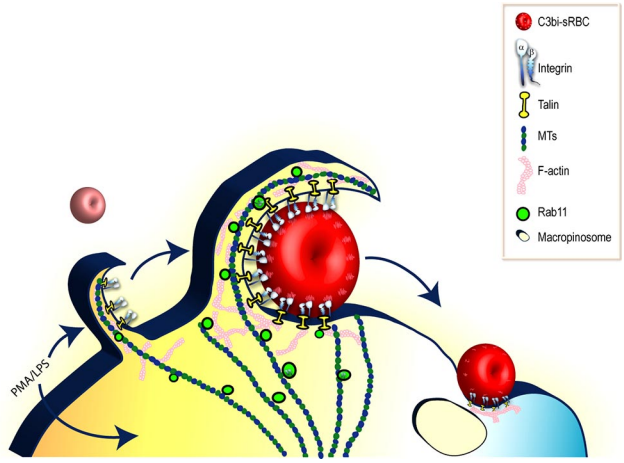

Figure 7. A model of membrane ruffle-mediated capture of C3bi-sRBCs in activated macrophages. After macrophage stimulation, F-actin–rich macropinocytosis membrane ruffles protrude by kinesin-mediated delivery of Rab11-containing recycling endosomes. Ruffle formation promotes accumulation of Mac-1 receptors and recruitment of talin to facilitate integrin clustering and activation within the ruffle. Amassed receptors within the ruffle promote adherence of approaching complement-opsonized particles. After particle attachment to the macrophage cell surface, ruffles collapse to form a macropinosome beneath the bound particle, after which the particle slowly "sinks" into the cytoplasm for maturation events.

DISCUSSION

In this study we demonstrate a functional link between macrophage activation, macropinocytosis, and Mac-1–mediated phagocytosis. Signals from PMA and LPS stimulate a variety of processes in macrophages beyond changes in integrin activity, and our results suggest the concomitant increase in macropinocytosis in activated macrophages (Swanson, 1989; Poussin *et al.*, 1998) allows these cells to more aggressively bind complement-coated particles. Macropinocytosis ruffles are large, actin-rich protrusions that are consequently structurally equipped to entangle large particles within a thin membrane veil. Many invasive bacteria are capable of evoking focal membrane ruffles at the site of attachment of target cells such as epithelial cells (Isberg, 1991; Bliska *et al.*, 1993). Binding of phosphatidylserine to macrophages also initiates macropinocytosis as a means to clear apoptotic cells (Hoffmann *et al.*, 2001). Our results show that activated macrophages similarly exploit macropinocytosis machinery to promote binding of C3bi-opsonized particles. Complement is a ubiquitous, highly conserved component of the innate immune system and macropinocytosis induced by inflammatory mediators may represent a widespread mechanism for uptake of complement-coated noninvasive bacteria or dying cells by activated macrophages.

We observed by SEM that both PMA- and LPS-induced macropinocytosis ruffles partially encircle C3bi-sRBCs in mouse and human macrophages. Membrane-ruffle capture of C3bi-sRBCs was most evident with higher doses of LPS, suggesting that encounters with whole bacterium, bacterial fragments, and/or septic conditions might ready macrophages for quick clearance of bacteria. On the basis of our results we propose a model where macrophage stimulation by inflammatory mediators or bacterial products signals to the cytoskeleton to promote actin remodeling and membrane extension, to drive ruffle formation (Figure 7). These findings are in agreement with recent observations of membrane protrusions observed around C3bi-sRBCs (Hall *et al.*, 2006). Early SEM studies identified membrane ruffles associated with C3bi-sRBCs (Kaplan, 1977; Aderem and Underhill, 1999); however, this finding was refuted by transmission electron microscopy analysis where only particle "sinking" was observed (Kaplan, 1977; Newman *et al.*, 1991; Allen and Aderem, 1996; Aderem and Underhill, 1999). These discrepancies may be due to different stages of phagocytosis analyzed or the techniques used for imaging the plasma membrane. One advantage of using SEM to study phagocytosis is that it provides a panoramic overview of surface remodeling events.

We further utilized live cell imaging strategies to more fully understand the nature and purpose of membrane ruffles during phagocytosis. Our live DIC imaging analysis revealed highly dynamic membrane ruffles that were induced after macrophage activation. As part of their sentinel function, activated macrophages may develop constitutive ruffles as a search-and-capture strategy for nearby opsonized particles. Based on our DIC movies, C3bi particles that made full contact with membrane ruffles were selectively captured. We consistently observed membrane ruffles associated with C3bi-sRBCs after washing and processing for SEM, suggesting that membrane ruffles promote particle adherence more strongly than other cell surface regions. The enrichment of actin and Mac-1 within the membrane ruffles strongly suggests that integrin avidity is modulated after macrophage activation. To our knowledge, this is the first description of receptor clustering during macropinocytosis, and is reminiscent of β1 integrin clustering observed in *Salmonella*-induced membrane ruffles (Garcia-del Portillo *et al.*, 1994). We also see enhanced staining for talin and the CBRM1/5 antibody within "empty" membrane ruffles, suggesting that macrophage activation signals modulate integrin affinity to engage the ruffles with C3bi particles. Ruffles containing active integrins may serve as an initial particle tethering mechanism after which outside-in signaling stimulates lateral mobilization of integrins to sites of bound particles. Mac-1 persists around C3bi particles during internalization (Figure 3A and Clemens and Horwitz, 1992; Allen and Aderem, 1996), indicating that a portion of the ruffle membrane remains associated with the particle during nascent phagosome formation or that further recruitment of Mac-1 occurs after particle capture.

Our results also provide an explanation for the strong requirement for MTs in both macropinocytosis and Mac-1–mediated phagocytosis, observed by ourselves and numerous groups (Newman *et al.*, 1991; Racoosin and Swanson, 1992; Allen and Aderem, 1996). We see MTs penetrating the core of membrane ruffles and actin-rich regions during C3bi-frustrated phagocytosis assays. Although MTs may be important for orchestrating actin dynamics within the membrane ruffle, we have evidence for a requirement for MT-mediated integrin delivery to the cell surface (Figure 7). We provide the first evidence for the cell surface delivery of integrins in macrophages stimulated with either PMA or LPS, which has a strong dependency on intact MTs. Taxol stimulation of macrophages caused a modest increase in ruffle formation, integrin clustering, and C3bi-particle binding, providing further correlation between these events and indicating that stabilized MTs are a key component behind ruffle formation in activated macrophages. However, ruffle formation and particle binding in taxol-stimulated cells did not reach the levels observed in activated macrophages, suggesting that PMA, LPS, and thioglycollate activate additional pathways to mediate these events. These additional pathways are potentially involved in integrin delivery to the cell membrane, which was not significantly up-regulated in

taxol-stimulated cells. The latter finding indicates that the MT-dependent integrin delivery to the cell surface depends on a dynamic MT subset in macrophages, whereas stable MTs contribute to actin remodeling and ruffle extension.

Membrane ruffle formation showed a complete dependency on intact MTs. Given the substantive size of the ruffle protrusion, it is not surprising that akin to pseudopod formation in FcγR-mediated phagocytosis, intracellular membrane stores are necessary for ruffle development. We observe Rab11-GFP–labeled vesicles associating with CLIP 170, a MT plus-end tracking protein, and anterograde delivery of these vesicles to membrane ruffles during C3bi-particle binding. Rab11 is also delivered to forming pseudopods during FcγR-mediated phagocytosis (Cox *et al.*, 2000), suggesting there may be a conservation of recruited membranes for plasma membrane extensions in phagocytosis in macrophages. Both kinesin inhibition and Rab11 DN expression reduce ruffle formation and C3bi-sRBC binding. We did not observe a role for Rab5 in C3bi-particle binding, which could be attributed to normal membrane ruffling in the presence of mutant Rab5, which has also been observed by others (Li *et al.*, 1997). However, Rab34 was essential for membrane ruffle formation and C3bi-particle binding. In light of evidence showing a key role for Rab34 in macropinocytosis and its localization to ruffles (Sun *et al.*, 2003), it is not unexpected that it is also involved in C3bi-particle adherence. Although it is not clear how Rab34 contributes to early macropinocytosis ruffles, there is accumulating evidence that Rab11 participates in targeted delivery of integrins to the cell surface (Powelka *et al.*, 2004; Yoon *et al.*, 2005). Mac-1 resides in secretory vesicles in neutrophils that are mobilized to the plasma membrane when neutrophils are activated with inflammatory mediators (Sengelov, 1995). In addition to supplying extra membrane for ruffle extension, MT-mediated trafficking of recycling endosomes to the site of ruffle formation may direct intracellular stores of integrins to facilitate particle adherence. We observed that a small subset of Mac-1 requires Rab11 for delivery to the cell surface during macrophage activation. It will be of interest to identify other intracellular pools of integrins that are mobilized in stimulated macrophages, and the cooperation of Rab34 in mediating integrin delivery/ruffle formation. Our results thus far are the first documentation of membrane delivery to sites of membrane ruffle formation and C3bi-particle attachment.

In summary, we have characterized a novel mechanism for binding of large complement-opsonized particles to the surface of macrophages. Although activated macrophages exploit macropinocytosis ruffles for particle adherence, the particles do not appear to be engulfed into the macropinosomes that form beneath the bound particles (Figure 7). Activated macrophages may only utilize the membrane ruffle portion of the macropinocytosis machinery to allow maximal exposure of concentrated receptors to particles. As internalization of C3bi-sRBCs is known to be a relatively slow process (Caron and Hall, 1998; Olazabal *et al.*, 2002), ruffle capture of particles may help more firmly adhere particles ,whereas additional actomyosin machinery assembles to eventually squeeze the particle into the cell. However, these studies do not rule out the possibility that fragments of the particle may be taken up into the newly formed macropinosome for antigen processing and presentation. Studies investigating further links between phagocytosis and macropinocytosis in activated macrophages may provide important insights into the sentinel function of cells of the innate immunity, for particulate antigen sampling of the environment.

ACKNOWLEDGMENTS

We thank Dr. J. Brumell (Hospital for Sick Children, Toronto) for the EGFP-Rab11 constructs and Dr. D. Arnold (University of Southern California) for the EGFP-Kif5B DN constructs. We acknowledge the kind gift of the EGFP-Rab5 DN and EGFP-Rab34 DN plasmids from Dr. S. Grinstein (Hospital for Sick Children, Toronto) and thank Dr. N. Galjart (Erasmus University Medical Center, Rotterdam, The Netherlands) for sharing CLIP-170 antibodies. We thank Dr. J. Jongstra-Bilen (University Health Network, Toronto) for providing mouse peritoneal and thioglycollate-elicited mouse macrophages. We also thank Dr. K. C. Kain and Ziyue Lue (University Health Network, Toronto) for TLR4$^{-/-}$ mouse macrophages and Dr. J. Booth and Dr. S. Gupta (Sunnybrook Health Science Centre, Toronto) for human monocyte-derived macrophages. We thank Payman Samavarchi-Tehrani for his assistance with DIC imaging and SEM analysis. We are grateful to Jenny Jongstra-Bilen as well as to James Booth and Mauricio Terebiznik for critical reading of the manuscript. R.E.H. is the recipient of an Ontario Early Researcher Award (ERA) and a Canadian Institutes for Health Research (CIHR) New Investigator Award and is supported by a CIHR grant and a National Science and Engineering Research Council (NSERC) grant.

REFERENCES

Aderem, A., and Underhill, D. M. (1999). Mechanisms of phagocytosis in macrophages. Annu. Rev. Immunol. *17*, 593–623.

Allen, L. A., and Aderem, A. (1996). Molecular definition of distinct cytoskeletal structures involved in complement- and Fc receptor-mediated phagocytosis in macrophages. J. Exp. Med. *184*, 627–637.

Bannerman, D. D., and Goldblum, S. E. (1999). Direct effects of endotoxin on the endothelium: barrier function and injury. Lab. Invest. *79*, 1181–1199.

Binker, M. G., Zhao, D. Y., Pang, S. J., and Harrison, R. E. (2007). Cytoplasmic linker protein-170 enhances spreading and phagocytosis in activated macrophages by stabilizing microtubules. J. Immunol. *179*, 3780–3791.

Bliska, J. B., Galan, J. E., and Falkow, S. (1993). Signal transduction in the mammalian cell during bacterial attachment and entry. Cell *73*, 903–920.

Caron, E., and Hall, A. (1998). Identification of two distinct mechanisms of phagocytosis controlled by different Rho GTPases. Science *282*, 1717–1721.

Clemens, D. L., and Horwitz, M. A. (1992). Membrane sorting during phagocytosis: selective exclusion of major histocompatibility complex molecules but not complement receptor CR3 during conventional and coiling phagocytosis. J. Exp. Med. *175*, 1317–1326.

Coquelle, F. M. *et al.* (2002). LIS1, CLIP-170's key to the dynein/dynactin pathway. Mol. Cell. Biol. *22*, 3089–3102.

Cox, D., Lee, D. J., Dale, B. M., Calafat, J., and Greenberg, S. (2000). A Rab11-containing rapidly recycling compartment in macrophages that promotes phagocytosis. Proc. Natl. Acad. Sci. USA *97*, 680–685.

Dersch, P., and Isberg, R. R. (1999). A region of the *Yersinia* pseudotuberculosis invasin protein enhances integrin-mediated uptake into mammalian cells and promotes self-association. EMBO J. *18*, 1199–1213.

Diamond, M. S., and Springer, T. A. (1993). A subpopulation of Mac-1 (CD11b/CD18) molecules mediates neutrophil adhesion to ICAM-1 and fibrinogen. J. Cell Biol. *120*, 545–556.

Dowrick, P., Kenworthy, P., McCann, B., and Warn, R. (1993). Circular ruffle formation and closure lead to macropinocytosis in hepatocyte growth factor/scatter factor-treated cells. Eur J. Cell Biol. *61*, 44–53.

Finlay, B. B., and Cossart, P. (1997). Exploitation of mammalian host cell functions by bacterial pathogens. Science *276*, 718–725.

Garcia-del Portillo, F., and Finlay, B. B. (1994). *Salmonella* invasion of nonphagocytic cells induces formation of macropinosomes in the host cell. Infect. Immun. *62*, 4641–4645.

Garcia-del Portillo, F., Pucciarelli, M. G., Jefferies, W. A., and Finlay, B. B. (1994). *Salmonella typhimurium* induces selective aggregation and internalization of host cell surface proteins during invasion of epithelial cells. J. Cell Sci. *107*(Pt 7), 2005–2020.

Griffin, F. M., Jr., and Mullinax, P. J. (1985). Effects of differentiation in vivo and of lymphokine treatment in vitro on the mobility of C3 receptors of human and mouse mononuclear phagocytes. J. Immunol. *135*, 3394–3397.

Hall, A. B., Gakidis, M. A., Glogauer, M., Wilsbacher, J. L., Gao, S., Swat, W., and Brugge, J. S. (2006). Requirements for Vav guanine nucleotide exchange factors and Rho GTPases in FcgammaR- and complement-mediated phagocytosis. Immunity *24*, 305–316.

Hoffmann, P. R., deCathelineau, A. M., Ogden, C. A., Leverrier, Y., Bratton, D. L., Daleke, D. L., Ridley, A. J., Fadok, V. A., and Henson, P. M. (2001).

Phosphatidylserine (PS) induces PS receptor-mediated macropinocytosis and promotes clearance of apoptotic cells. J. Cell Biol. *155*, 649–659.

Hughes, P. E., and Pfaff, M. (1998). Integrin affinity modulation. Trends Cell Biol. *8*, 359–364.

Isberg, R. R. (1991). Discrimination between intracellular uptake and surface adhesion of bacterial pathogens. Science *252*, 934–938.

Jones, B. D., Paterson, H. F., Hall, A., and Falkow, S. (1993). *Salmonella typhimurium* induces membrane ruffling by a growth factor-receptor-independent mechanism. Proc. Natl. Acad. Sci. USA *90*, 10390–10394.

Jongstra-Bilen, J., Harrison, R., and Grinstein, S. (2003). Fcgamma-receptors induce Mac-1 (CD11b/CD18) mobilization and accumulation in the phagocytic cup for optimal phagocytosis. J. Biol. Chem. *278*, 45720–45729.

Kaplan, G. (1977). Differences in the mode of phagocytosis with Fc and C3 receptors in macrophages. Scand. J. Immunol. *6*, 797–807.

Khandani, A., Eng, E., Jongstra-Bilen, J., Schreiber, A. D., Douda, D., Samavarchi-Tehrani, P., and Harrison, R. E. (2007). Microtubules regulate PI-3K activity and recruitment to the phagocytic cup during Fcgamma receptor-mediated phagocytosis in nonelicited macrophages. J. Leukoc. Biol. *82*, 417–428.

Li, G., D'Souza-Schorey, C., Barbieri, M. A., Cooper, J. A., and Stahl, P. D. (1997). Uncoupling of membrane ruffling and pinocytosis during Ras signal transduction. J. Biol. Chem. *272*, 10337–10340.

Lim, J., Wiedemann, A., Tzircotis, G., Monkley, S. J., Critchley, D. R., and Caron, E. (2007). An essential role for talin during alpha(M)beta(2)-mediated phagocytosis. Mol. Biol. Cell *18*, 976–985.

Newman, S. L., Mikus, L. K., and Tucci, M. A. (1991). Differential requirements for cellular cytoskeleton in human macrophage complement receptor- and Fc receptor-mediated phagocytosis. J. Immunol. *146*, 967–974.

Olazabal, I. M., Caron, E., May, R. C., Schilling, K., Knecht, D. A., and Machesky, L. M. (2002). Rho-kinase and myosin-II control phagocytic cup formation during CR, but not FcgammaR, phagocytosis. Curr. Biol. *12*, 1413–1418.

Phaire-Washington, L., Silverstein, S. C., and Wang, E. (1980). Phorbol myristate acetate stimulates microtubule and 10-nm filament extension and lysosome redistribution in mouse macrophages. J. Cell Biol. *86*, 641–655.

Poussin, C., Foti, M., Carpentier, J. L., and Pugin, J. (1998). CD14-dependent endotoxin internalization via a macropinocytic pathway. J. Biol. Chem. *273*, 20285–20291.

Powelka, A. M., Sun, J., Li, J., Gao, M., Shaw, L. M., Sonnenberg, A., and Hsu, V. W. (2004). Stimulation-dependent recycling of integrin beta1 regulated by ARF6 and Rab11. Traffic *5*, 20–36.

Racoosin, E. L., and Swanson, J. A. (1992). M-CSF-induced macropinocytosis increases solute endocytosis but not receptor-mediated endocytosis in mouse macrophages. J. Cell Sci. *102*(Pt 4), 867–880.

Ratnikov, B. I., Partridge, A. W., and Ginsberg, M. H. (2005). Integrin activation by talin. J. Thromb. Haemost. *3*, 1783–1790.

Ross, G. D., and Vetvicka, V. (1993). CR3 (CD11b, CD18): a phagocyte and NK cell membrane receptor with multiple ligand specificities and functions. Clin. Exp. Immunol. *92*, 181–184.

Sanchez-Mejorada, G., and Rosales, C. (1998). Signal transduction by immunoglobulin Fc receptors. J. Leukoc. Biol. *63*, 521–533.

Schmidt, A., Caron, E., and Hall, A. (2001). Lipopolysaccharide-induced activation of beta2-integrin function in macrophages requires Irak kinase activity, p38 mitogen-activated protein kinase, and the Rap1 GTPase. Mol. Cell. Biol. *21*, 438–448.

Sengelov, H. (1995). Complement receptors in neutrophils. Crit. Rev. Immunol. *15*, 107–131.

Simonson, W. T., Franco, S. J., and Huttenlocher, A. (2006). Talin1 regulates TCR-mediated LFA-1 function. J. Immunol. *177*, 7707–7714.

Sun, P., Yamamoto, H., Suetsugu, S., Miki, H., Takenawa, T., and Endo, T. (2003). Small GTPase Rah/Rab34 is associated with membrane ruffles and macropinosomes and promotes macropinosome formation. J. Biol. Chem. *278*, 4063–4071.

Swanson, J. A. (1989). Phorbol esters stimulate macropinocytosis and solute flow through macrophages. J. Cell Sci. *94*(Pt 1), 135–142.

Swanson, J. A., and Watts, C. (1995). Macropinocytosis. Trends Cell Biol. *5*, 424–428.

Tjelle, T. E., Lovdal, T., and Berg, T. (2000). Phagosome dynamics and function. Bioessays *22*, 255–263.

van Kooyk, Y., and Figdor, C. G. (2000). Avidity regulation of integrins: the driving force in leukocyte adhesion. Curr. Opin. Cell Biol. *12*, 542–547.

Vidarsson, G., and van de Winkel, J. G. (1998). Fc receptor and complement receptor-mediated phagocytosis in host defence. Curr. Opin. Infect. Dis. *11*, 271–278.

Williams, L. M., and Ridley, A. J. (2000). Lipopolysaccharide induces actin reorganization and tyrosine phosphorylation of Pyk2 and paxillin in monocytes and macrophages. J. Immunol. *164*, 2028–2036.

Williams, M. A., and Solomkin, J. S. (1999). Integrin-mediated signaling in human neutrophil functioning. J. Leukoc. Biol. *65*, 725–736.

Wright, S. D., and Griffin, F. M., Jr. (1985). Activation of phagocytic cells' C3 receptors for phagocytosis. J. Leukoc. Biol. *38*, 327–339.

Wright, S. D., and Silverstein, S. C. (1982). Tumor-promoting phorbol esters stimulate C3b and C3b' receptor-mediated phagocytosis in cultured human monocytes. J Exp. Med. *156*, 1149–1164.

Yoon, S. O., Shin, S., and Mercurio, A. M. (2005). Hypoxia stimulates carcinoma invasion by stabilizing microtubules and promoting the Rab11 trafficking of the alpha6beta4 integrin. Cancer Res. *65*, 2761–2769.